

A Nanometer-Sized High-Spin Polyradical: Poly(4-phenoxy-1,2-phenylenevinylene) Planarily Extended in a Non-Kekulé Fashion and Its Magnetic Force Microscopic Images

Hiroyuki Nishide,* Takahiro Ozawa, Makoto Miyasaka, and Eishun Tsuchida

Contribution from the Department of Polymer Chemistry, Waseda University, Tokyo 169-8555, Japan

Received August 7, 2000

Abstract: A π -conjugated, but non-Kekulé- and nondisjoint-type poly(1,2-phenylenevinylene) network bearing 4-substituted di-*tert*-butylphenoxy groups was synthesized through a one-pot polycondensation of the star-shaped subpart and the subsequent oxidation, which was persistent even at room temperature. The polyphenoxy radical with a spin concentration of 0.4 displayed an average S of 10/2. The polyradical with the molecular weight of 3.2×10^4 gave a disklike image of ca. 35×0.6 nm with both an atomic and a magnetic force microscopy: the molecular image was examined as a nanoscale and single-molecular-based magnetic dot.

Introduction

Recent advances in nanotechnology have strongly stimulated the research efforts focused on new materials with sizes from one to several tens of nanometer(s). For example, particles with a nanometer-size and consisting of metals are being developed as a magnetic dot where, e.g., quantum effects are taken into account.¹ On the other hand, the electronic, optical, and magnetic functions of organic molecules have been studied and utilized at a macroscopic bulk level or as condensed materials, while their functions are essentially ascribed to their activities at the molecular level. A nanoscale material design by covalently extending the organic-based functional molecules will be a good methodology to create nanometer-sized functional materials,² since their size and shape are controlled, maintaining their well-defined chemical structure, by conventional organic chemical approaches. The extended and up-sized molecules, i.e., very high molecular weight polymers, possess single-molecular-based sizes in the nanometer-range, and the nanometer-sizes of such covalently extended molecules are kept even after being dispersed as an isolated single molecule on a substrate or embedded in an ultrathin coating. Therefore, they are expected to open up possibilities that are absent in either conventional subnanosized molecules or macroscopic materials and, in nanoscale studies, a scanning probe microscopy³ has been found to be an effective tool.

Due to the possibility of obtaining purely organic-derived magnetic materials, there has been recent interest in the synthesis of high-spin polyradical molecules based on exchange coupling through a π -conjugated bond.^{4,5} Rajca et al. demonstrated a very high-spin alignment with a spin quantum number (S) of ca. 20/2 by precisely synthesizing dendritic-macrocyclic poly(1,3-phenylenephenylmethine)s based on the radicals being cross-conjugatively formed in the backbones.^{5a–c} An increase in the molecular size of the polyradicals, however, always accompanies the formation of a spin defect and a decrease in the through-bond interactions between a large number of spin sites within the molecule. Thus multiple coupling pathways of the spin sites or a two-dimensionally π -conjugated network bring(s) about a significant increase in S for such polyradical molecules. Rajca et al. eventually succeeded in reporting the highest recorded value of spin alignment for purely organic molecules, with an average S of $\geq 80/2$ at a low temperature, on the highly cross-linked network of macrocyclic units; the network with a molecular weight of 10^4 was prepared by the condensation of two elegantly designed and tetrafunctionalized calix[4]arene derivatives.⁶

In contrast to the backbone conjugatively connected radicals developed by Rajca et al., a π -conjugated polymer pendantly bearing multiple radical groups in a non-Kekulé and nondisjoint^{4d,7} fashion has only recently been studied as another approach to

(1) (a) Hehm, M.; Ounadjela, K.; Bucher, J.-P.; Rousseux, F.; Decanini, D.; Bartenlian, B.; Chappert, C. *Science* **1996**, 272, 1782. (b) Fernandez, A.; Gibbons, M. R.; Wall, M. A.; Cerjan, C. J. *J. Magn. Magn. Mater.* **1998**, 190, 71. (c) Li, S. P.; Lew, W. S.; Xu, Y. B.; Hirohata, A.; Samad, A.; Baker, F.; Bland, J. A. C. *Appl. Phys. Lett.* **2000**, 76, 748. (d) Sun, S.; Murray, C. B.; Weller, D.; Folks, L.; Moser, A. *Science* **2000**, 287, 1989.

(2) (a) Carter, F. L. *Molecular Electronic Devices*; Marcel Dekker: New York, 1982. (b) Aviram, A.; Ratner, M., Eds. *Molecular Electronics: Science and Technology*; Annals of the New York Academy of Sciences, No. 852; New York Academy of Sciences: New York, 1998. (c) Gimzewski, J. K.; Joachim, C. *Science* **1999**, 283, 1683. (d) Schlüter, A. D.; Rabe, J. P. *Angew. Chem., Int. Ed.* **2000**, 39, 864. (e) Kunitake, T.; Nakahama, S.; Takahashi, S.; Toshima, N., Eds. *Precision Polymers and Nano-Organized Systems*; Kodansha: Tokyo, 2000.

(3) (a) DiNard, N. J. *Nanoscale Characterization of Surfaces and Interfaces*; VCH: Weinheim, 1994. (b) Sarid, D. *Scanning Force Microscopy*; Oxford University Press: New York, 1994. (c) Bottomley, L. A. *Anal. Chem.* **1998**, 70, 425R.

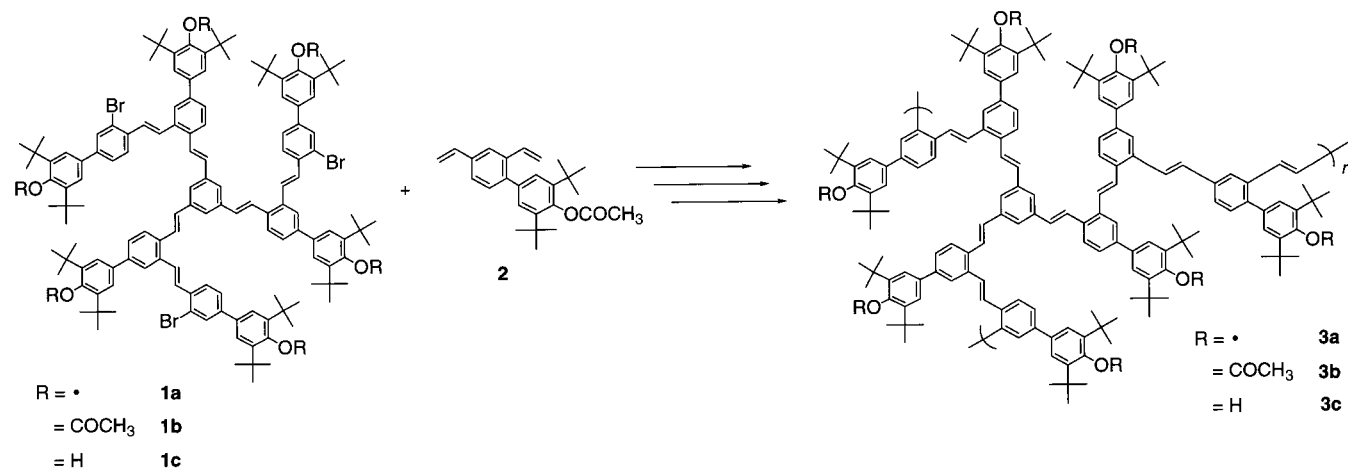
(4) (a) Dougherty, D. A. *Acc. Chem. Res.* **1991**, 24, 88. (b) Iwamura, H.; Koga, N. *Acc. Chem. Res.* **1993**, 26, 346. (c) Rajca, A. *Chem. Rev.* **1994**, 94, 871. (d) Lahti, P. M. *Magnetic Properties of Organic Materials*; Marcel Dekker: New York, 1999.

(5) (a) Rajca, A.; Lu, K.; Rajca, S. *J. Am. Chem. Soc.* **1997**, 119, 10355. (b) Rajca, A.; Wongsriratanakul, J.; Rajca, S. *J. Am. Chem. Soc.* **1997**, 119, 11674. (c) Rajca, A.; Wongsriratanakul, J.; Rajca, S.; Cerny, R. *Angew. Chem., Int. Ed. Engl.* **1998**, 37, 1229. (d) Bushby, R. J.; Gooding, D. J. *Chem. Soc., Perkin Trans. 2* **1998**, 1069. (e) Anderson, K. K.; Dougherty, D. A. *Adv. Mater.* **1998**, 10, 688. (f) Sedo, J.; Ventosa, N.; Ruiz-Molina, D.; Mas, M.; Molins, E.; Rovira, C.; Veciana, J. *Angew. Chem., Int. Ed. Engl.* **1998**, 37, 330. (g) Shultz, D. A.; Boal, A. K.; Farmer, G. T. *J. Org. Chem.* **1998**, 63, 9462. (h) Xie, C.; Lahti, P. M. *J. Polym. Sci. A* **1999**, 37, 779. (i) Shultz, D. A.; Bodnar, S. H.; Krishna Kumar, R. *J. Am. Chem. Soc.* **1999**, 121, 10664.

(6) Rajca, A.; Rajca, S.; Wongsriratanakul, J. *J. Am. Chem. Soc.* **1999**, 121, 6308.

(7) Borden, T.; Davidson, E. R. *J. Am. Chem. Soc.* **1977**, 99, 4587.

Chart 1



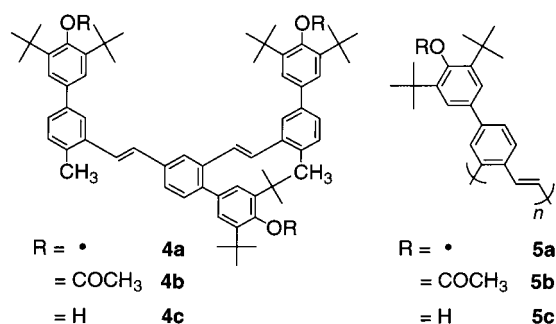
the very high-spin molecules.^{4d,8} The advantages of the pendant-type polyradicals to realize a very high-spin and durable molecule are as follows: the introduction of a chemically persistent radical group as a pendant spin source, insensitivity to spin defects, and a long distance interaction to align even remote spins. We recently synthesized a linear (**5**) and a star-shaped poly(1,2-phenylenevinylene) bearing a 4-substituted di-*tert*-butylphenoxy as the pendant group and have reported a through-conjugated backbone bond and long-range ferromagnetic exchange interaction between the pendant polyphenoxy spins.^{8,9}

We have, in this study, successfully extended the pendant polyradicals to a π -conjugated but non-Kekulé-type network structure (**3a** in Chart 1) by satisfying the nondisjoint and ferromagnetic connectivity of the multiple pendant spin sites. We used the one-step polycondensation of a trifunctionalized subpart (**1b**) and a bifunctionalized subpart (**2**) under a dilute [**1b**]/[**2**] = 4/3 condition to yield a polymer with a molecular size in the nanometer-range and the ferromagnetic connectivity. The resultant high-spin polyphenoxy radical **3a** had substantial stability and was easily handled, e.g., at room temperature and in air. Such feasibility and the nanoscale molecular size have, for the first time, enabled a magnetic force microscopy (MFM) analysis of an organic polyradical molecule. We will demonstrate a single-molecular-based magnetic dot image of the high-spin organic polyradical.

Results and Discussion

The star-shaped hexamer subpart **1b** was synthesized by selectively reacting the iodo position of 1,3,5-triiodobenzene, as the core of the star-shaped structure, with the vinyl group of 2-bromo-2'-vinyl-4,5'-bis(3,5-di-*tert*-butyl-4-acetoxyphenyl)stilbene via the Heck reaction using a catalyst of palladium acetate and tri-*o*-tolylphosphine. **1** is a smaller part of our previously reported star-shaped octet polyradical⁹ and possesses three bromide groups at the end of each 1,2-phenylenevinylene arm. The symmetrical structure of **1b** or **1c** was supported by 30 peaks in the ¹³C NMR spectrum, the ¹H-¹H-COSY and HMQC spectra of the aromatic region (see Experimental Section and Supporting Information), and a strong blue fluorescence at 450

Chart 2



nm and IR of 962 cm⁻¹ ($\delta_{\text{HC=CH}}$) attributed to the *trans*-stilbene moieties. 4-(3,5-Di-*tert*-butylacetoxyphenyl)-1,3-divinylbenzene **2** was prepared by introducing the 3,5-di-*tert*-butyl-4-trimethylsilyloxyphenyl group onto 4-bromo-1,3-xylene, and the two methyl groups were modified into two vinyl groups.

The ferromagnetic coupling capability of **2** was examined by synthesizing a model quartet molecule **4** (Chart 2). The reaction of **2** and 2-bromo-4-(3,5-di-*tert*-butyl-4-acetoxyphenyl)-toluene using the Pd-phosphine catalyst (under the same reaction conditions for the polycondensation to be described later) quantitatively yielded **4b**. The precursor **4b** was hydrolyzed and oxidized⁹ to give the triradical **4a**. Magnetization of **4a** in frozen 2Me-THF was measured using a SQUID magnetometer. The normalized magnetization plots (M/M_s) of the triradical **4a** were very similar to the Brillouin curve for $S = 3/2$ at 1.8–5 K (see Figure 2): this indicates a quartet ground state of the triradical **4a** and that the cross-linking structure part of **3a** satisfies the non-Kekulé and nondisjoint connectivity between the radical groups (i.e., nonbonding molecular orbitals of **4a** share the same molecular region that enhances the ferromagnetic spin-exchange interaction⁷).

The trifunctionalized star-shaped subpart **1b** and the bifunctionalized subpart **2** were reacted in the feed ratio of [**1b**]/[**2**] = 4/3 using the Pd-phosphine catalyst ([Pd]/[**1** + **2**] = 1/10) under dilute conditions ([**1b** + **2**] = 0.01 M in DMF) at 90 °C for 5 days. The polymer **3b** was obtained as a yellow powder and was quite soluble in common solvents such as benzene, THF, and chloroform despite its poly(phenylenevinylene) skeleton and cross-linked structure. The molecular weight of the polymer was estimated to be 3.2×10^4 based on a light-scattering measurement.¹⁰ Flory¹¹ has clearly described that the polycondensation of a trifunctionalized unit A₃ and a bifunctionalized unit B₂ with the feed ratio [A₃]/[B₂] = 4/3 yields a

(8) (a) Nishide, H.; Kaneko, T.; Nii, T.; Katoh, K.; Tsuchida, E.; Yamaguchi, K. *J. Am. Chem. Soc.* **1995**, *117*, 548. (b) Nishide, H.; Kaneko, T.; Nii, T.; Katoh, K.; Tsuchida, E.; Lahti, P. M. *J. Am. Chem. Soc.* **1996**, *118*, 9695.

(9) (a) Nishide, H.; Miyasaka, M.; Tsuchida, E. *Angew. Chem., Int. Ed. Engl.* **1998**, *37*, 2400. (b) Nishide, H.; Miyasaka, M.; Tsuchida, E. *J. Org. Chem.* **1998**, *63*, 7399.

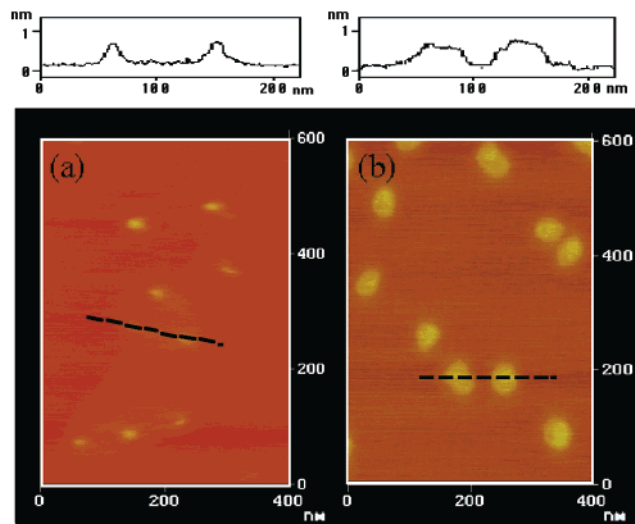


Figure 1. AFM images (tapping mode) of the precursor polymers **1c** (a) and **3c** (b), with a molecular weight of 2.2×10^3 and 3.2×10^4 , respectively.

polymer with an infinite molecular weight and terminal A groups. The bromide content of **3b** determined by elemental analysis was consistent with the structure of **3b** based on the bromide (or **1b**) terminals and the molecular weight (degree of polymerization of **1** and **2** units = 15; the phenolic moiety number within the molecule = 90). The polycondensation at the feed ratio $[\mathbf{1b}]/[\mathbf{2}] > 4/3$ gave only an oligomer, e.g., **3b** with the molecular weight of 5.0×10^3 from the polycondensation at the feed ratio of $[\mathbf{1b}]/[\mathbf{2}] = 2$. On the other hand, the polycondensation at the feed ratio of $[\mathbf{1b}]/[\mathbf{2}] = 1$ and/or in a nondiluted solution ($[\mathbf{1b} + \mathbf{2}] = 0.1$ M) resulted in gelation.

3b was hydrolyzed for over one week to give **3c**. The dilute dichloromethane solution of **3c** was transferred to a highly oriented pyrolytic graphite (HOPG) surface and subjected to atomic force microscopy (AFM) (Figure 1). The horizontal distance of ca. 35 and ca. 5 nm was estimated for **3c** and **1c** with the molecular weight of 3.2×10^4 and 2.2×10^3 , respectively, by taking into account the cantilever tip in a tapping mode.¹² This size corresponded to the molecular weight of the polymer. In contrast, the vertical distance of ca. 0.6 nm was estimated for both **3c** and **1c**. These images suggested a pseudo-two-dimensionally extended and planar disklike shape for the polymer **3**.

The ionization potential (threshold, I^{th}) was estimated by ultraviolet photoelectron spectroscopy. The I^{th} values of **1c**, **3c**, and the corresponding linear hydroxy polymer of **5** (molecular weight 2.4×10^4) were 6.0₀, 5.8₄, and 5.8₈ eV, respectively;¹³ the I^{th} value significantly decreased through the extension of **1c** to **3c**, which indicates a highly extended π -conjugation for **3**.

3c was converted to the polyphenoxyl radical **3a**. **3a** was isolated as a brownish green powder which was persistent at room temperature even in air (half-life = 1.2 days¹⁴).

(10) The number-average (M_n) and weight-average molecular weight (M_w) were 3.2×10^4 and 3.8×10^4 , respectively ($M_w/M_n = 1.2$).

(11) Flory, P. J. *J. Am. Chem. Soc.* **1941**, *63*, 3083.

(12) A silicon cantilever (Digital Instruments Inc.: length 125 μm , width 30 μm , and thickness 3–5 nm with a spring constant between 20 and 100 N/m) was used. The tip used for Figure 1 was a commercial one (Digital Instruments Inc. NCH: tip height was 10–15 μm and the radius curvature at the front was ca. 5 nm). Resonance peaks in the frequency response of the cantilever were selected in the range between 280 and 320 kHz for the tapping mode oscillation. A horizontal resolution of the images was hardly affected by the tip species.

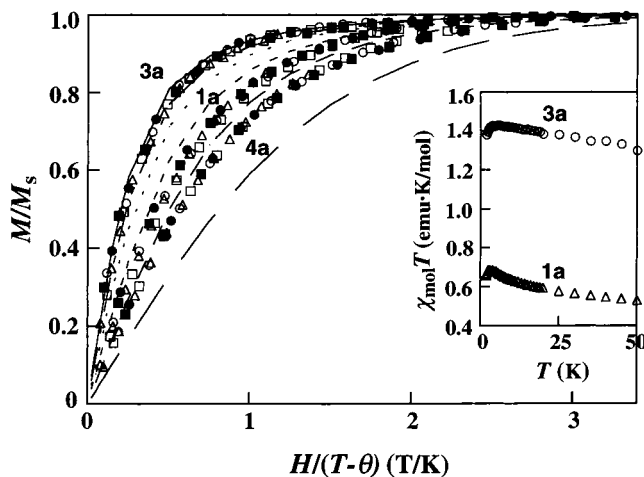


Figure 2. Normalized plots of magnetization (M/M_s) vs the ratio of magnetic field and temperature ($H/(T - \theta)$) for **3a**, **1a**, and **4a** with a spin concentration of 0.42, 0.75, and 0.80 spin/phenol residue, respectively, in 2Me-THF at $T = 1.8$ (\bullet), 2.0 (\blacksquare), 2.5 (\circ), 3 (\square), and 5 (Δ) K, and the theoretical curves corresponding to the $S = 1/2, 3/2, 5/2, 7/2, 9/2, 11/2$ Brillouin functions. $\theta = -0.07, -0.05$, and -0.02 K for **3a**, **1a**, and **4a**, respectively. Inset: $\chi_{\text{mol}}T$ vs T plots for **3a** and **1a**. χ_{mol} was estimated using χ measured at $H = 0.5$ T and the spin concentration.

The normalized magnetization (M/M_s) plots of the polyphenoxyl **3a** with a spin concentration of 0.42 spin/phenol residue were close to the Brillouin curve for $S = 10/2$ (Figure 2).^{15,16} Unfortunately, only ca. 40% of the potential spin-sites were successfully oxidized to the phenoxyl radicals; however, the S value was much higher than that for the small star-shaped subpart with a spin concentration of 0.75 ($S = 4/2$). The extended network acted as an effective π -conjugated coupler of the pendant spins.

Magnetic force microscopy (MFM) was applied to study both the molecular image and the magnetic response of the high-spin polyphenoxyl radical **3a**. MFM is almost the same method as AFM, except for the use of a magnetized tip.^{3,17} The first scan is in a tapping mode to recognize the surface (AFM with a magnetized tip), and the second scan in the same area uses a noncontact mode (with ca. 20 nm above the surface in this experiment) to monitor the local magnetization of the sample.

The dilute dichloromethane solution of **3a** (molecular weight = 3.2×10^4) was transferred to a HOPG surface and subjected to AFM (Figure 3a), followed by MFM (Figure 3b). The AFM gave a ca. 35 nm-sized image of the high-spin polyphenoxyl molecule, similar to the precursor **3c** in Figure 1b. The following

(13) I^{th} was estimated on the polymer films using a UPS spectrometer (Riken Keiki: AC-1). Reference data were measured using the same procedure for poly(1,2-phenylenevinylene) and poly(acetylene): $I^{\text{th}} = 6.17$ and 5.2₅, respectively.

(14) The half-life of the polyradical was estimated using the time-course of the integrated ESR intensity of the sample standing at room temperature in air.

(15) The plots of the product of molar magnetic susceptibility (χ_{mol}) and T vs T are shown in the inset of Figure 2. The plots lie close to the expected $\chi_{\text{mol}}T$ values, 1.5 and 0.75 emu·K/mol for **3a** and **1a**, respectively, at 4 K, and slightly decrease at both lower and higher temperatures. The former is probably ascribed to a weak through-space antiferromagnetic interaction. The latter (or very slight $\chi_{\text{mol}}T$ decrease with temperature increase, especially for **3a**) suggests a relatively strong spin-exchange coupling in the polyradicals.

(16) The best preparation of **3a** (spin concentration = 0.42) gave an average S of 10/2 (Figure 2). **3a** (spin concentration 0.36) gave an average S of 8/2.

(17) (a) Bending, S. J. *Adv. Phys.* **1999**, *48*, 449. (b) Scholl, A. *Science* **2000**, *288*, 1762. (c) Heinze, S.; Bode, M.; Kubetzka, A.; Pietzsch, O.; Nie, X.; Blügel, S.; Wiesendanger, R. *Science* **2000**, *288*, 1805.

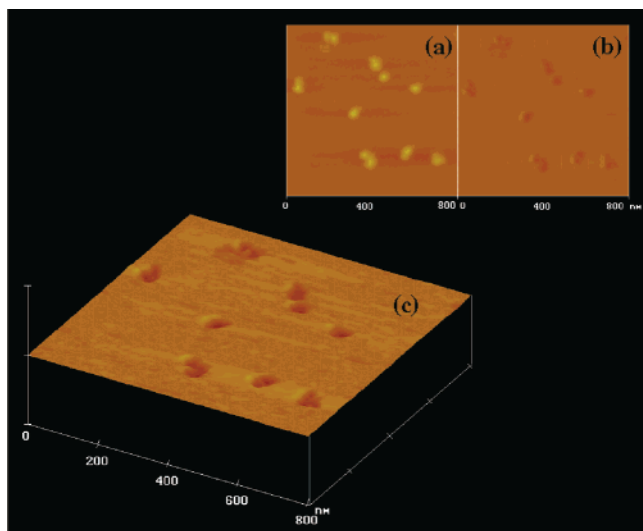


Figure 3. Force microscopy images of the polyradical **3a** with a molecular weight of 3.2×10^4 : (a) the AFM image, (b) the MFM image obtained immediately after AFM in the same scan area, (c) the 3D-MFM topography, and (d–f) force microscopy images of **3a** taken under the same conditions as Figure 3a–c, except using a MFM tip magnetized in the opposite direction of Figure 3a–c.

MFM clearly indicated a magnetic gradient response exactly on the molecular position. The three-dimensional representation of the MFM topography (Figure 3c) demonstrates “holes” ascribed to the magnetic molecules or an attraction of the magnetized MFM tip to the polyradicals. This MFM image was reversed when the tip was magnetized in the opposite direction (Figure 3f). The MFM images of the polyradical molecule disappeared after the measurement for ca. 1 day, which corresponded to inactivation of the radical under ambient conditions.¹⁸

A dichloromethane solution of the polyradical **3a** and diamagnetic polystyrene was spin-coated on a substrate (the

(18) Although the MFM image of the polyradical disappeared after ca. 1 day, the AFM molecular image remained intact even after the complete disappearance of the MFM image (after 1 week). While the precursor polymer **3c** on HOPG provided the AFM image shown in Figure 1, the precursor **3c** did not give any magnetic gradient response in any scan area of the MFM measurement. Similar MFM images were obtained for the polyradical **3a** prepared via the oxidation of **3c** with lead oxide. These results support the fact that radical generation is necessary to produce the MFM image. The MFM contrast was weakened with the decrease in the spin concentration and hardly detectable for the polyradical with a spin concentration of 0.1.

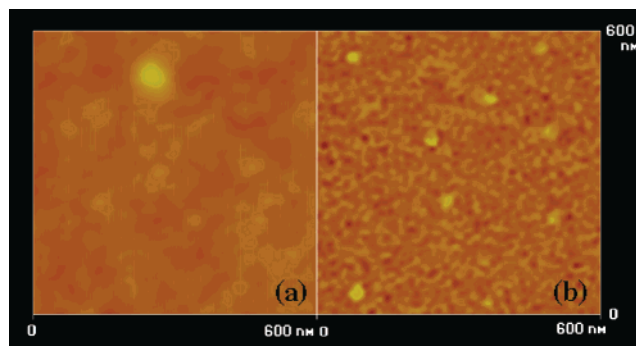


Figure 4. Force microscopy images of the polyradical **3a** with a molecular weight of 3.2×10^4 embedded in a polystyrene coating with a thickness of 5 nm: (a) the AFM image and (b) the MFM image obtained immediately after AFM in the same scanning area.

coating thickness was 5 nm). The flat surface of the coating was supported by the monotonic AFM image (Figure 4a). On the other hand, MFM produced dots in the image (Figure 4b), of which the size almost coincided with the molecular size of **3a**; the MFM tip interacted with the polyradical molecules embedded in the polystyrene thin coating. MFM did not respond, e.g., to any defect or dust of the coating (e.g., in the upper edge of Figure 4a), but did respond to the local magnetization of the coating. The MFM image of Figure 4b was maintained for one week, which is ascribed to the prolonged lifetime of the radical embedded in a glassy polystyrene coating. These results suggest that MFM is an effective tool to detect a very weak magnetic signal of such high-spin organic polymers and that the polyradical molecule is a potentially new material of nanosized and molecular-based magnetic dots.

Experimental Section

Synthetic Procedure. 1,3,5-Tris[2'-styryl-2''-bromo-{5',4''-bis(3,5-di-*tert*-butyl-4-acetoxyphenyl)stilbene}]benzene (1b**).** Palladium acetate (22.9 mg, 0.102 mmol), tri-*o*-tolylphosphine (62.1 mg, 0.204 mmol), and triethylamine (1.03 g, 10.2 mmol) were added to a DMF (4.1 mL) solution of 2-bromo-2'-vinyl-4,5'-bis(3,5-di-*tert*-butyl-4-acetoxyphenyl)stilbene (see the Supporting Information) (0.600 g, 0.771 mmol) and 1,3,5-triiodobenzene (0.114 g, 0.250 mmol). The solution was warmed to 45 °C for 64 h, cooled to room temperature, and extracted with CHCl₃. The organic layer was evaporated and the crude product was purified by silica gel column separation with a hexane/CHCl₃ (1/3) eluent to give a pale yellow powder of **1b**: yield 16%; ¹H NMR (CDCl₃, 500 MHz, ppm) δ 1.37 (s, 108H, *tert*-butyl), 2.38 (s, 18H, –O–CO–CH₃), 7.16–7.80 (m, 45H, Ar, –HC=CH–); ¹³C NMR (CDCl₃, ppm) δ 22.67, 31.47, 35.59, 124.57, 125.01, 125.21, 125.38, 126.35, 126.57, 127.10, 127.32, 129.25, 130.50, 131.20, 131.63, 134.94, 135.77, 136.21, 136.31, 137.76, 138.36, 140.44, 142.52, 143.00, 147.76, 148.06, 171.02, 171.14; IR (KBr pellet, cm⁻¹) 1765 (ν_{C=O}), 962 (δ_{transHC=CH}); FAB-MS (*m/z*) 2405.8 (found), calcd for *M* = 2405.7; correct elemental analysis.

4-(3,5-Di-*tert*-butyl-4-acetoxyphenyl)-1,3-divinylbenzene (2**).** **2** was prepared in the same manner as above via the Wittig reaction: yield 30%; ¹H NMR (CDCl₃, 500 MHz, ppm) δ 1.36 (s, 18H, *tert*-butyl), 2.37 (s, 3H, –O–CO–CH₃), 5.21 (d, 1H, 11 Hz, –CH=CH₂), 5.28 (d, 1H, 11 Hz, –CH=CH₂), 5.70 (d, 1H, 17 Hz, –CH=CH₂), 5.80 (d, 1H, 17 Hz, –CH=CH₂), 6.73 (dd, 1H, 11 Hz, 17 Hz, –CH=CH₂), 6.77 (dd, 1H, 11 Hz, 17 Hz, –CH=CH₂), 7.22–7.41 (m, 5H, Ar, –HC=CH–); ¹³C NMR (CDCl₃, ppm) δ 22.73, 31.52, 35.56, 114.06, 114.65, 124.10, 125.24, 128.02, 128.11, 130.33, 136.13, 136.48, 136.65, 137.04, 140.44, 141.85, 147.03, 171.09; IR (KBr pellet, cm⁻¹) 1763 (ν_{C=O}), 1628 (ν_{C=C}); MS (*m/z*) 376 (*M*⁺), calcd for *M* = 376.5.

Polymerization. Palladium acetate (1.3 mg, 5.81 μmol), tri-*o*-tolylphosphine (3.54 mg, 11.6 μmol), triethylamine (58.8 mg, 0.581 mmol), and **2** (9.38 mg, 24.9 μmol) were added to a DMF solution (5.69 mL) of **1b** (80 mg, 32.0 μmol) (molar feed ratio **1b**/**2** = 4/3).

The solution was heated at 90 °C for 5 days. The polymer was purified by reprecipitating twice from CHCl₃ in methanol to yield a yellow powder of **3b**: yield 64%; ¹H NMR (CDCl₃, 500 MHz; ppm) δ 1.36 (s, 126H, *tert*-butyl), 2.35 (s, 21H, -O-CO-CH₃), 7.16–7.84 (m, 39H, Ar, -HC=CH-); IR (KBr pellet, cm⁻¹) 1764 (ν_{C=O}), 961 (δ_{transHC=CH}); molecular weight = 3.2 × 10⁴ (the ratio of weight-average and number-average molecular weight = 1.2); bromide content = 4.5%, as determined by the combustion method; UV-vis λ_{max} = 320 nm; fluorescence at 450 nm (λ_{ex} = 320 nm) ascribed to the *trans*-stilbene structure.

3b was deprotected in the DMSO solution of excess aqueous KOH for 7 days to yield **3c**: yield 68%; ¹H NMR (CDCl₃, 500 MHz; ppm): δ 1.43 (s, 126H, *tert*-butyl), 5.21 (s, 7H, OH), 7.09–7.93 (m, 39H, Ar, -HC=CH-); IR (KBr pellet, cm⁻¹): 3636 (ν_{O-H}), 961 (δ_{transHC=CH}); Molecular weight = 3.2 × 10⁴ (the ratio of weight-average and number-average molecular weight = 1.2).

4-(3,5-Di-*tert*-butylacetoxyphenyl)-*m*-bis(2'-methyl-5'-(3'',5''-di-*tert*-butylacetoxyphenyl))benzene (4b). **4b** was prepared via the Heck reaction of **2** (1 equiv) and 2-bromo-4-(3,5-di-*tert*-butyl-4-acetoxyphenyl)toluene (2.2 equiv): yield 80%; ¹H NMR (CDCl₃, 500 MHz, ppm) δ 1.41 (s, 54H, *tert*-butyl), 2.36 (s, 9H, -O-CO-CH₃), 2.42 (s, 6H, -CH₃), 7.22–7.84 (m, 19H, Ar, -HC=CH-); ¹³C NMR (CDCl₃, ppm) δ 19.67, 22.73, 31.51, 35.51, 124.69, 124.81, 125.34, 125.44, 126.62, 126.74, 126.93, 127.02, 128.07, 128.34, 128.57, 130.09, 130.38, 130.61, 130.77, 134.60, 134.76, 136.53, 136.71, 136.86, 136.91, 137.17, 138.35, 138.41, 139.82, 139.98, 140.70, 142.08, 142.35, 142.49, 142.64, 147.08, 147.37, 147.46, 171.05; IR (KBr pellet, cm⁻¹) 1763 (ν_{C=O}), 966 (δ_{transHC=CH}); FAB-MS (*m/z*) 1049.6 (found), calcd for *M* = 1049.5.

Preparation of the Polyradicals. An aqueous sodium hydroxide (1 mL, 20 equiv to the phenol) was added to a 2Me-THF solution (2 mL) of **3c** (20 unit mM), and the solution was stirred for 0.5 h under a nitrogen atmosphere. The solution was then vigorously stirred with 1 mL of aqueous potassium ferricyanide (20 equiv to the phenolate) at room temperature. The solution turned dark green after 0.5–1 h, which was ascribed to the phenoxyl radical formation. The organic layer was washed with water and dried over anhydrous sodium sulfate to give a solution of **3a**, **1a**, **4a**, and **5a** were prepared in the same manner from **1c**, **4c** (for their syntheses, see Supporting Information), and **5c**,⁸ respectively. The dichloromethane solution of **3c** was similarly prepared for the AFM and MFM measurements.

Magnetic Measurement. The **3c** dissolved in 2Me-THF was heterogeneously oxidized with an alkaline potassium ferricyanide under an inert atmosphere. The solution of the phenoxyl polymer was immediately transferred to a diamagnetic plastic capsule after the oxidation. The magnetization and static magnetic susceptibility were measured with a Quantum Design MPMS-7 SQUID magnetometer. The magnetization was measured from 0.1 to 7 T at 1.8, 2.0, 2.5, 3,

and 5 K. The static magnetic susceptibility was measured from 2 to 200 K in a field of 0.5 T. Ferromagnetic magnetization ascribed to the impurities was determined by the Honda-Owen plots to be very low (<1 ppm) and subtracted from the overall magnetization. Diamagnetic susceptibility (-1.3 × 10⁻⁷ emu) of the sample solution and the diamagnetic capsule was estimated by the Curie plots of magnetic susceptibility, which almost agreed with the value calculated with Pascal's constant of the solvent. The corrected magnetization data were fitted to Brillouin functions using a self-consistent version of the mean field approximation.

AFM and MFM Measurements. A drop of 1–5 μM dichloromethane solution of the polyradical **3c** was transferred onto a freshly cleaved HOPG using a microsyringe, and the solvent was carefully blotted off by air-drying. If a concentrated solution was used, the polymer was aggregated on the surface. The AFM and MFM experiments were performed using a Nanoscope III (Digital Instruments Inc.). The cantilever used in the MFM experiment was a commercial one (NANOPROBE SPM TIPS Type MESP) containing a tip thinly coated with ferromagnetic CoCr with a length of 225 μm and a magnetic moment of 10⁻¹³ emu. The MFM images in the noncontact mode were obtained immediately after AFM in the tapping mode in the same scan area with a scan rate of 2 Hz, a drive resonance frequency of ca. 78 kHz, and a scan lift height of 20 nm, which were selected upon tuning.

Acknowledgment. This work was partially supported by Grants-in-Aid for Scientific Research (No. 12555268) and COE Program "Molecular Nano-Engineering" from the Ministry of Education, Science and Culture, Japan, and by the NEDO R&D Project on Technology for Novel High-Functional Materials.

Supporting Information Available: Syntheses and characterization of 2-iodo-4-(3,5-di-*tert*-butyl-4-trimethylsiloxyphenyl)toluene, 2-iodo-4-(3,5-di-*tert*-butyl-4-hydroxyphenyl)toluene, 2-iodo-4-(3,5-di-*tert*-butyl-4-acetoxyphenyl)toluene, 2-bromo-2'-methyl-4,5'-bis(3,5-di-*tert*-butyl-4-acetoxyphenyl)-stilbene, 1,3,5-tris[2'-styryl-2''-bromo-{5',4''-bis(3,5-di-*tert*-butyl-4-hydroxyphenyl)stilbene}]benzene (**1c**), 4-(3,5-di-*tert*-butyl-4-trimethylsiloxyphenyl)-*m*-xylene, 4-(3,5-di-*tert*-butyl-4-hydroxyphenyl)-*m*-xylene, 4-(3,5-di-*tert*-butyl-4-acetoxyphenyl)-*m*-xylene, and 4-(3,5-di-*tert*-butylhydroxyphenyl)-*m*-bis(2'-methyl-5'-(3'',5''-di-*tert*-butylhydroxyphenyl))benzene (**4c**) (PDF). This material is available free of charge via the Internet at <http://pubs.acs.org>.

JA002944U